

UDC

TOPOLOGICAL ANALYSIS OF THE BONDING IN $[\text{Ru}_5(\mu_4\text{-C}_2)\text{L}(\text{CO})_{13}]$
AND $[\text{Ru}_4(\mu_4\text{-C}_2)\text{L}(\text{CO})_{10}]$ COMPLEXES ($\text{L} = (\mu\text{-SMe})(\mu\text{-PPh}_2)_2$)

© 2012 A. May, N. Ouddai*

*Laboratoire Chimie des matériaux et des vivants: Activité, Réactivité, Université El-Hadj Lakhdar, Batna, Algérie**Received July, 8, 2010**С доработки — March, 23, 2011*

The nature of metal-metal and metal-carbon bonding interactions within the penta- and tetra-ruthenium acetylide complexes $[\text{Ru}_5(\mu_4\text{-C}_2)\text{L}(\text{CO})_{13}]$ (**1**) and $[\text{Ru}_4(\mu_4\text{-C}_2)\text{L}(\text{CO})_{10}]$ (**2**) respectively are investigated using the present topological theories of the chemical bond: AIM and ELF. The electron density analysis within the framework of Atoms in Molecules (AIM) indicates that, in the first complex, only one bond path exists between the Ru4 and Ru5 metal atoms, whereas there is no direct bonding between ruthenium atoms in the second complex. On the other hand, the ELF analysis reveals that in both complexes, all Ru—C bonds belong to closed-shell type interactions and leads to the conclusion that the Ru—Ru bond is predominantly covalent. Moreover, the presence of trisynaptic basins in the first complex points out a three-center bond connecting ruthenium atoms.

Key words: topological analysis, Atoms in Molecules (AIM), electron localization function (ELF), metal acetylide.

INTRODUCTION

Metal acetylide complexes are of both theoretical and practical interest, in particular, as their potential to form molecular wires [1–3], liquid crystals [4], electrical conductors [5], and other nanoelectronic devices [6, 7]. In this context, Chris J. Adams et al. [8] reported the synthesis and structural determination of penta- and tetra-ruthenium acetylide complexes $[\text{Ru}_5(\mu_4\text{-C}_2)\text{L}(\text{CO})_{13}]$ (**1**) and $[\text{Ru}_4(\mu_4\text{-C}_2)\text{L}(\text{CO})_{10}]$ (**2**) respectively, where L denotes the $(\mu\text{-SMe})(\mu\text{-PPh}_2)_2$ group.

The acetylide ligand C_2 in complex (**1**) (Fig. 1, *a*) bridges one edge of the Ru_3 core and the isolated Ru—Ru bonded fragment in a $\mu, \mu\text{-}\eta^1, \eta^2$ mode, albeit with asymmetric Ru— C_2 π interactions [8], whereas that of (**2**) bridges all the four metal atoms (Fig. 1, *b*).

The first attempts to address theoretically the bonding properties in these compounds, in practical within the subunit Ru_5C_2 of (**1**) and Ru_4C_2 of (**2**), are due to the work of Frapper and Halet [9] who used a EH calculation and the effective atomic number formalism. Depending on whether the acetylide ligand acts as a four- or six-electron donor, this method provides two tautomeric forms for (**1**) (Fig. 2, *a, b*) and at least three others for (**2**) (Fig. 2, *c–e*).

In order to further probe the bonding rearrangement of this complexes, two methods that have proved to be less arbitrary than the traditional Mulliken population based schemes were employed [10]: atoms in molecules (AIM) and the electron localization function (ELF).

The main goal of the present study is to examine topologically the possible existence and the nature of each metal-metal and metal— $\text{C}_{(\text{acetylide})}$ bond, combining the AIM theory with the analysis of the ELF.

* E-mail: Ouddai_nadia@yahoo.fr

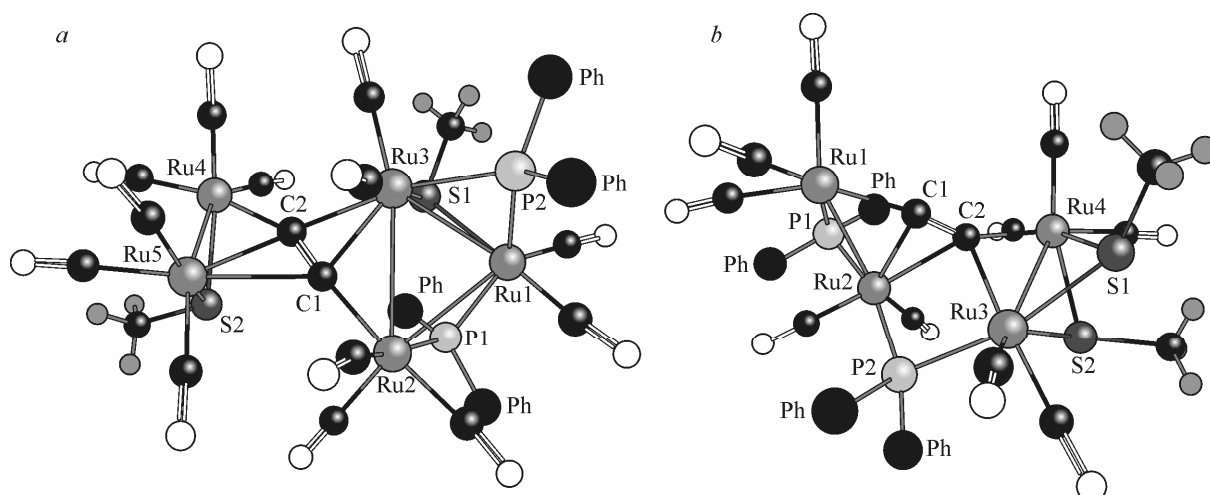


Fig. 1. Structure of (1) (a); structure of (2) (b).
For clarity the phenyl group was replaced by a dummy atom Ph

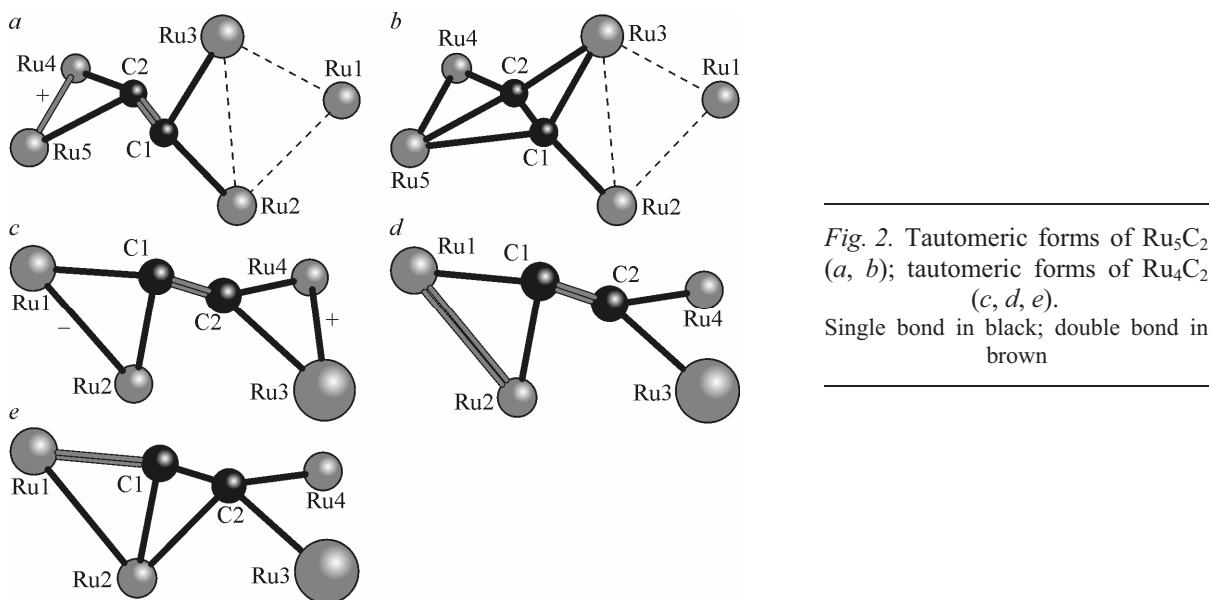


Fig. 2. Tautomeric forms of Ru₅C₂ (a, b); tautomeric forms of Ru₄C₂ (c, d, e).
Single bond in black; double bond in brown

COMPUTATIONAL METHODOLOGY

All DFT calculations were carried out using the Amsterdam Density Functional (ADF) program package [11]. To get the best relation between a reliable model and computer time, the total structure was reduced only to a minimal degree [12]: the phenyl rings were replaced by four hydrogen atoms. The geometry of each simplified model, [Ru₅(μ₄-C₂)L'(CO)₁₃] and [Ru₄(μ₄-C₂)L'(CO)₁₀], L'=(μ-SMe)(μ-PH₂)₂, were fully optimized at LDA [13], PB86 [14] and BLYP [15] levels of theory. Triple-ζ Slater-type valence orbitals (STO) augmented by one set of polarization functions (TZP) were used for all atoms, with the core orbital being kept frozen throughout; [1s] cores of C and O, [1s-2p] core of P and S, and [1s-4p] core of Ru. Relativistic effects have been considered at the scalar level using the method of zeroth-order regular approximation (ZORA) [16]. The X-ray atomic coordinates of both complexes (1) and (2) were obtained from the Cambridge Crystallographic Data Center (CCDC) with reference codes REXPIT [8] and REXPOZ [8] respectively.

The topological analysis of ELF and of the electron density according to Bader's Atoms in Molecules (AIM) scheme was performed using the DGrid/Basin program [17]. The molecular structure, molecular graphs, and ELF isosurfaces were achieved by the Chemcraft 1.4 program [18].

Table 1

Selected bond lengths (\AA) and bond angles (deg.) of complex (1')

Bonds	Exp [8]	LDA	PB	BLYP
Ru1—Ru2	3,087	3,112	3,232	3,312
Ru1—Ru3	2,956	3,013	3,09	3,14
Ru2—Ru3	3,17	3,159	3,249	3,332
Ru4—Ru5	2,694	2,696	2,738	2,773
Ru2—C1	2,06	2,056	2,097	2,13
Ru3—C1	2,27	2,23	2,318	2,383
Ru3—C2	2,47	2,395	2,534	2,62
Ru4—C2	2,13	2,04	2,09	2,12
Ru5—C1	2,65	2,488	2,664	2,757
Ru5—C2	2,34	2,254	2,332	2,382
C1—C2	1,2	1,283	1,283	1,279
Ru4—C1—C2	172	168,74	172,031	172,781
Ru4—C2—C1	155	151,393	154,565	156,272

Table 2

Selected bond lengths (\AA) and bond angles (deg.) of complex (2')

Bonds	Exp [8]	LDA	PB	BLYP
Ru1—Ru2	2,796	2,839	2,914	2,949
Ru2—Ru3	3,571	3,561	3,7	3,769
Ru3—Ru4	3,13	3,165	3,236	3,31
Ru1—C1	2,027	1,993	2,029	2,057
Ru2—C1	2,28	2,286	2,354	2,395
Ru2—C2	2,499	2,493	2,608	2,666
Ru3—C2	2,325	2,265	2,316	2,369
Ru4—C2	2,135	2,1	2,137	2,172
C1—C2	1,239	1,279	1,285	1,281
Ru1—Ru2—Ru3	95,06	93,57	91,448	91,062
Ru2—Ru3—Ru4	77,98	76,046	76,419	76,425

RESULTS AND DISCUSSION

Calculated structures: The key geometry parameters calculated at LDA, BP86, and BLYP levels are listed in Tables 1, 2 together with the experimental data on complexes (1) and (2) for comparison. For the first complex (Table 1), the LDA values of the ruthenium-to-ruthenium bond distances are close to the experimental ones, whilst the ruthenium-to-carbon bond lengths are better described by the PB86 method. For the acetylide moiety, it appears that the gradient correction in GGA does not improve the C=C bond distance prediction over that of LDA. For the second complex (Table 2), the ruthenium-to-ruthenium and ruthenium-to-carbon distances predicted by the calculations using the local (LDA) functional agree remarkably well with the experimental values. In addition, the bond length of the acetylide moiety is well reproduced by all the calculation methods.

Thus, from the above results both LDA and PB86 approaches are a reasonable chemical model to study the molecular structure of our complexes. However, in order to overcome the less accurate description of some geometrical parameters provided by these methods, only the data corresponding to the experimental structure will be considered.

Bonding analysis. The electronic structure resulting from the PB86/ZORA/TZP calculations of experimental simplified models was analyzed in terms of the AIM theory and complementarily, through the ELF distribution.

For the experimental simplified models used in the benchmark calculations, each phenyl ring was exchanged by one hydrogen atom, but all geometrical parameters were kept fixed, except P—H bond lengths that were optimized using the PB86/ZORA/TZP level of theory. Since the ELF interpretation is sometimes obscured by the use of pseudopotentials or the frozen core approximation [19], the calculations of ELF were made at the all-electron level. Due to the fact that the metal-metal and metal-carbon_(acetylide) bonds are the major scope of this study, only the topological properties of Ru_5C_2 and Ru_4C_2 subunits of (1) and (2) respectively are discussed.

AIM analysis: The topological analysis of the electron density $\rho(r)$ based on Bader's AIM theory allows a quantitative description of bonds, nonbonding interactions, electronic structure, and reactivity [20]. In this theory, the existence of a chemical bond between an atom pair is conditioned to the appearance of a bond critical point (BCP) [21].

The nature of this bond can be described by the value of the electron density $\rho(r)$ and the Laplacian of the electron density $\nabla^2\rho(r)$. Thus, an unshared-electron interaction or closed shell interaction, as found in noble gas repulsive states, ionic bonds, hydrogen bonds, and van der Waals molecules, is

Table 3

Topological Properties (in a.u.) at Ru—Ru, Ru—C, and C=C BCPs of the Ru₅C₂ moiety

Bond critical point	Bonds	$\rho(r)$	$\nabla^2\rho(r)$	$ V /G$	$H(r)$
bcp1	Ru4—Ru5	0.056	0.074	1.449	-0.015
bcp 2	Ru4—C2	0.097	0.226	1.342	-0.029
bcp 3	Ru5—C2	0.061	0.138	1.273	-0.1
bcp 4	C1—C2	0.433	-1.464	3.436	-0.621
bcp 5	Ru3—C1	0.069	0.168	1.271	-0.015
bcp 6	Ru2—C1	0.110	0.260	1.359	-0.036

Table 4

Topological Properties (in a.u.) at Ru—Ru, Ru—C, and C=C BCPs of the Ru₄C₂ moiety

Bond critical point	Bond	$\rho(r)$	$\nabla^2\rho(r)$	$ V /G$	$H(r)$
bcp 1	Ru1—C1	0.1195	0.292	1.372	-0.043
bcp 2	Ru2—C1	0.069	0.167	1.281	-0.0163
bcp 3	C1—C2	0.400	-1.253	3.418	-0.530
bcp 4	Ru3—C2	0.060	0.149	1.242	-0.0115
bcp 5	Ru4—C2	0.096	0.204	1.363	-0.0293

characterized by low values of $\rho(r)$ and positive values of $\nabla^2\rho(r)$, whereas high values of $\rho(r)$ and negative $\nabla^2\rho(r)$ is unambiguously related to the covalent bond.

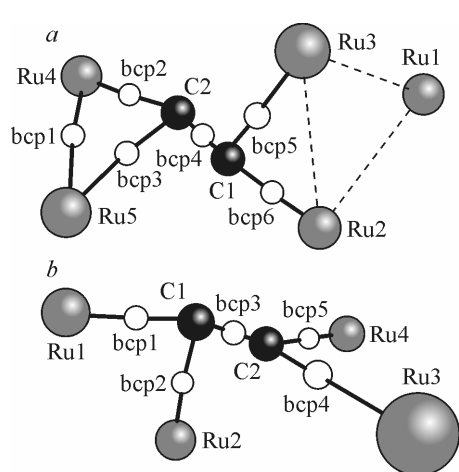
Tables 3, 4 summarize the local properties ($\rho(r)$, $\nabla^2\rho(r)$, $|V|/G$ and $H(r)$) computed at the BCPs found for both complexes, whereas the molecular graphs are shown in Fig. 3, a, b.

In the Ru₅C₂ moiety, Ru4—Ru5 BCP is characterized by a $\rho(r)$ value of 0.0561 a.u. and a $\nabla^2\rho(r)$ value of 0.0744 a.u. These values (a low electron density and a positive Laplacian) are often observed for bonds involving metal atoms and are a typical of the unshared-electron interaction [22]. It is now recognized that the distinction between the shared and unshared interactions based on $\nabla^2\rho(r)$ at BCP, though proven useful for bonding between the first row atoms, is not sufficient when heavier atoms are involved [20].

A better description can be based on other properties such as the kinetic energy density $G(r_c)$, the total electron energy density $H(r_c)$, and the ratio of these quantities to $\rho(r)$ [24]. The Laplacian $\nabla^2\rho(r)$ is linked to the kinetic energy density $G(r_c)$ (everywhere positive) and to the potential energy density $V(r_c)$ (everywhere negative) at each point r by a local virial theorem [22]. Both properties show different behavior in different bond types and are therefore used in topological analyses of transition metal complexes [24].

According to the sign of the total electron energy density $H(r_c)$ at BCP, Espinosa et al. divided the atomic interaction into three classes [25—29]: class I that corresponds to pure closed-shell interactions ($\rho(r) < 0.07$, $\nabla^2\rho(r) > 0$, $H(r_c) > 0$, $|V|/G < 1$) and class III that corresponds to pure covalent interactions ($\rho(r) > 0.15$, $\nabla^2\rho(r) < 0$, $H(r_c) < 0$, $|V|/G > 2$); class II is related to intermediate interactions ($0.07 < \rho(r) < 0.15$, $\nabla^2\rho(r) < 0$, $H(r_c) < 0$, $1 < |V|/G < 2$).

According to the above criteria, the characteristics of the Ru4—Ru5 bond allow us to assign them to the intermediate closed shell type (class II). In contrast, no such critical points are found between the other metallic centers. With reliance still on Bader's



criteria [30], the absence of this type of critical points between each two metal centers implies the lack of a direct metal-metal interaction. The four BCPs at the Ru—C bonds are located halfway between the Ru and C atoms and are characterized, also, by relatively small $\rho(r)$ values, positive $\nabla^2\rho(r)$ values, and negative $H(r_c)$. These BCP parameters correspond also to the intermediate closed shell type interaction. The $\rho(r)$ value is related to the bond order and can be considered a measure of the bond strength in such a way that the larger $\rho(r)$

Fig. 3. Molecular Graph of the Ru₅C₂ moiety (a) and molecular graph of the Ru₄C₂ moiety (b); bond paths (light blue), BCPs (red)

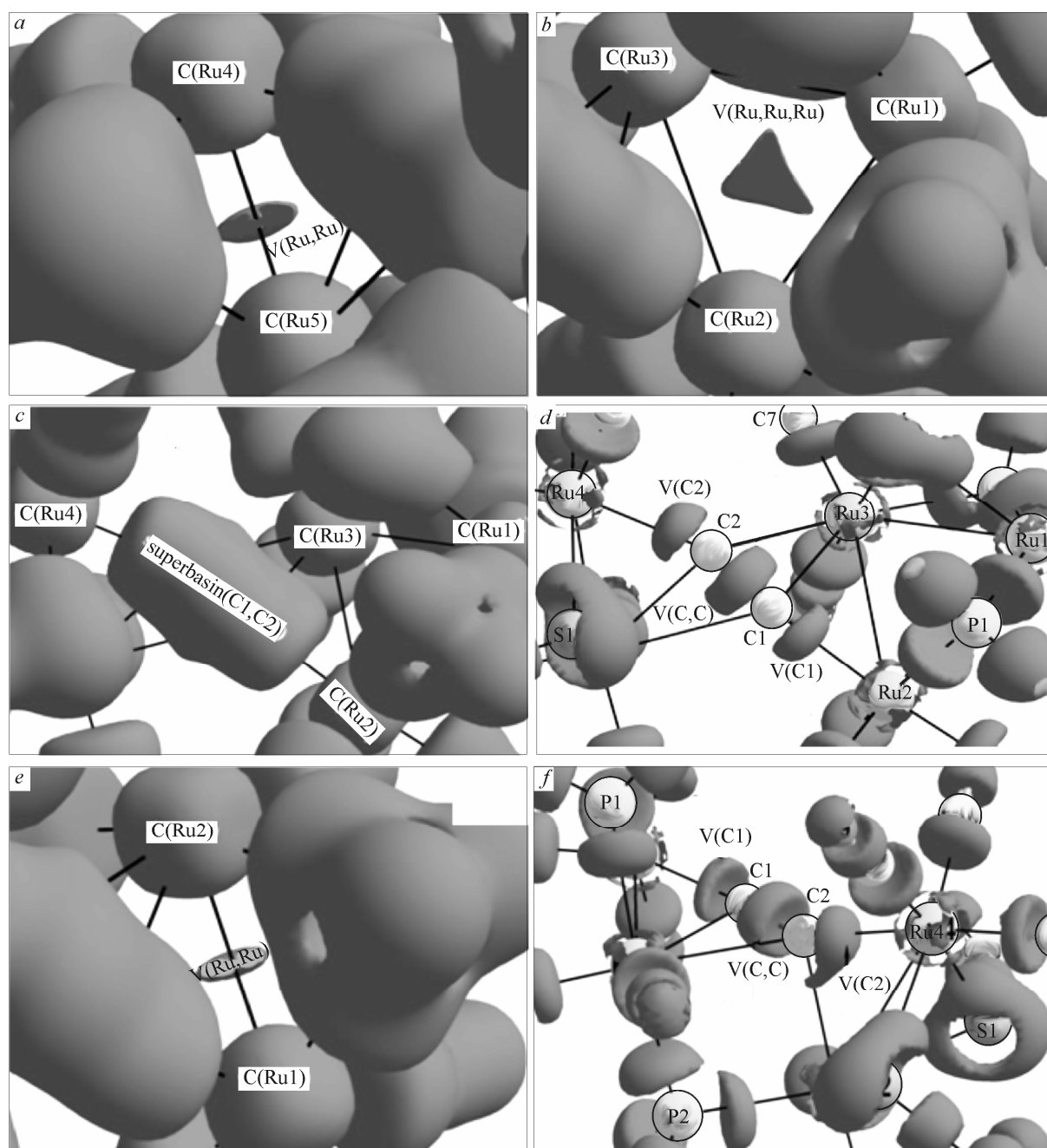


Fig. 4. ELF isosurfaces: ELF=0.3 for Ru_5C_2 showing the disynaptic basin $V(\text{Ru}_4,\text{Ru}_5)$ (a), the trisynaptic basin $V(\text{Ru}_1,\text{Ru}_2,\text{Ru}_3)$ (b), and the superbasin (C_1, C_2) (c); ELF=0.6 for Ru_5C_2 showing the bifurcation of the superbasin into $V(\text{C}_1)$, $V(\text{C}_2)$ and $V(\text{C},\text{C})$ (d); ELF=0.3 for Ru_4C_2 showing the disynaptic basin $V(\text{Ru}_1,\text{Ru}_2)$ (e); and ELF=0.6 for Ru_4C_2 showing the bifurcation of the superbasin into $V(\text{C}_1)$, $V(\text{C}_2)$ and $V(\text{C},\text{C})$ (f)

is, the stronger the bond [31]. The strength of each $\text{Ru}-\text{C}$ bond increases in the order $\text{Ru}_2-\text{C}_1 > \text{Ru}_4-\text{C}_2 > \text{Ru}_3-\text{C}_1 > \text{Ru}_5-\text{C}_2$. The molecular graph of Ru_4C_2 (Fig. 3, b) shows five BCPs (four $\text{Ru}-\text{C}$ and one $\text{C}-\text{C}$). The parameters of $\text{Ru}-\text{C}$ BCPs (Table 4) characterize the interaction of Ru and C atoms as an intermediate closed shell interaction too, and its strength increases in the order $\text{Ru}_1-\text{C}_1 > \text{Ru}_4-\text{C}_2 > \text{Ru}_2-\text{C}_1 > \text{Ru}_3-\text{C}_2$. However, the most important point is that the Ru_4C_2 moiety does not exhibit any BCPs between ruthenium atoms. This is suggestive of the absence of an interaction between these atoms. For $(\text{C}=\text{C})_{(\text{acetylide})}$ bonds, and in both complexes, the values of $\nabla^2\rho(r)$

Table 5

ELF basin properties for the Ru₅C₂ moiety

Basins	$\eta(r)$	$\rho(r)$	DIST ^a (Å°)	ECCNT ^b (Å°)
V(Ru4,Ru5)	0.450	30.042	1.46—1.46	0.57
V(Ru1,Ru2,Ru3)	0.4907	34.762	1.81—1.75—1.86	0.36
V(C1,C2)	0.9121	64.093	0.68—0.68	0.32
V(C1)	0.9274	55.611	0.66	—
V(C2)	0.9145	62.501	1.81—178—185	0.39

^a DIST shows the distance to the particular neighbors.

^b The eccentricity: perpendicular distance to the atom1—atom2 line.

The $\rho(r)$ values are given in atomic units; the ELF function $\eta(r)$ is adimensional.

(large and negative) are indicative of shared interactions, characterized by a large accumulation of charge between the nuclei. The bond ellipticity for this bond (0.04 in (1) and 0.05 in (2)) is closer to zero, consistent with the cylindrical symmetry of the BCP electron density usually associated with triple bonds [20, 32].

ELF analysis: Another complementary electron-density-based topological analysis which provides useful information on the bond structure is the electron localization function (ELF), as defined by Becke and Edgecombe [33]. The ELF topological analysis provides a partition of the molecular space in basins, which is consistent with the assumptions of Lewis theory [34]. These basins are either core basins surrounding a nucleus or valence basins that do not include a nucleus (except for protonated valence basins that include a proton). The number of connections of a given valence basin with the core basins is called the synaptic order. A disynaptic valence basin corresponds to a two-center bond, whereas a monosynaptic one corresponds to a lone pair or a group of lone pairs. Multi-center bonds, such as three-center two-electron (3c-2e) bonds, are taken into account by polysynaptic basins [35]. The presence of a di- or polysynaptic basin is usually indicative of a shared interaction of electrons (covalent, dative, or metallic bonds), while its absence usually denotes a closed-shell interaction (ionic, van der Waals, or hydrogen bond) [36].

In the Ru₅C₂ subunit, a topological analysis of ELF reveals a disynaptic basin V(Ru, Ru) located away from the Ru4—Ru5 bond line by 0.57Å° (Fig. 4, *a*), which has a small value of ELF (0.450), Table 5. The bond of this basin would be described as a covalent bond. Additionally, Fig. 4, *b* clearly shows the presence of a trisynaptic basin localized at a distance of 0.36 Å from the center of the triangular plane formed by the three atoms: Ru1, R2, and Ru3. The occurrence of the trisynaptic basin V(Ru1,Ru2,Ru3) clearly suggests a certain Ru1—Ru2—Ru3 three-centre bond in the molecule.

The ELF plots displayed in Fig. 4, *c* clearly show the presence of a superbasis, encompassing the acetylide fragment and detached entirely from the rest of the molecule. Bifurcation at ELF = 0.6 (Fig. 4, *d*), divides the superbasis into one disynaptic basin V(C1,C2), corresponding to the C1—C2 bond, and two monosynaptic basins V(C1) and V(C2) close to its corresponding carbon atoms and directed towards Ru2 and Ru4 atoms respectively. Thus, the binding between the Ru and C atoms belongs to the closed-shell type because no disynaptic basin is observed in the Ru—C bonding region. On other hand, the shape of the V(C1,C2) basin is similar to that of the ethyne molecule where for ELF = 0.8 the isosurface has a shape of a torus [37]. Hence, the somewhat torus shape of the C₂ bond basins is associated with a bond multiplicity of three, which is in good agreement with the above AIM finding.

The results of Table 6 and Fig. 4, *e, f* show that the topological analysis of the ELF function for the Ru₄C₂ subunit of complex (2) does not formally possess trisynaptic basins, but has five other basins; namely, two monosynaptic basins representing C valence electrons pairs, two disynaptic valence basins V(Ru, Ru), and V(C,C), corresponding to Ru1—Ru2 and C1—C2 bonds respectively.

Table 6

ELF basin properties for the Ru₄C₂ moiety

Basins	$\eta(r)$	$\rho(r)$	DIST ^a (Å°)	ECCNT ^b (Å°)
V(Ru1,Ru2)	0.4008	46.415	1.52—1.57	0.668
V(C1,C2)	0.9051	67.340	0.65—068	0.25
V(C1)	0.9166	93.292	0.65—0.65	0.27
V(C2)	0.9009	55.908	0.67	—

^a DIST shows the distance to the particular neighbors.

^b The eccentricity: perpendicular distance to the atom1—atom2 line.

The $\rho(r)$ values are given in atomic units; the ELF function $\eta(r)$ is adimensional.

CONCLUSIONS

From the topological analysis performed, we propose that there are six two-center bonds: four ruthenium-carbon, one ruthenium-ruthenium, and a triple carbon-carbon bond.

The properties of critical points in the region of Ru—Ru and Ru—C bonds clearly indicate the dominant role of the intermediate closed-shell interaction, whereas the valence type bond is evidently the C1—C2 bond.

From the point of view of the ELF topology, the nature of the Ru—C bond can be described as the closed-shell interaction characterized by the absence of any disynaptic attractor along the bond line; however, covalent Ru—Ru is also present. Furthermore, the ELF analysis supports the description obtained by AIM indicating the presence of a C—C_(acetylide) triple bond in both studied species.

REFERENCES

1. Bartik T., Bartik B., Brady M. et al. // *Angew. Chem.* – 1996. – **108**, N 4. – P. 467; *Chem., Int. Ed. Engl.* – 1996. – **35**, N 4. – P. 414.
2. Coat F., Lapinte C. // *Organometallics.* – 1996. – **15**, N 2. – P. 477.
3. Stang P.J., Ykwinski R.T. // *J. Amer. Chem. Soc.* – 1992. – **114**, N 11. – P. 4411.
4. Kaharu T., Ishii R., Adachi T. et al. // *J. Mater. Chem.* – 1995. – **5**, N 4. – P. 687.
5. (a) Irwin M.J., Gia G., Payne N.C., Puddephatt J. // *Organometallics.* – 1996. – **15**, N 1. – P. 51; (b) Shio-tsuka M., Yamamoto Y., Okuno S. et al. // *J. Chem. Soc. Chem. Commun.* – 2002. – N 6. – P. 590.
6. Long N. // *Angew. Chem.* – 1995. – **107**, N 1. – P. 37; *Angew. Chem., Int. Ed. Engl.* – 1995. – **34**, N 1. – P. 21.
7. Marder T., Fyfe H., Mlekuz M. et al. In: *Inorganic and Organometallic Polymers with Special Properties* / Laine. Ed. NATO. ASI. 206 and Kluwer – Dordrecht, 1992.
8. Adams C.J., Bruce M.I., Skelton B.W. et al. // *J. Chem. Soc., Dalton Trans.* – 1997. – N 3. – P. 371.
9. Frapper G., Halet J.-F. // *Organometallics.* – 1995. – **14**, N 11. – P. 5044.
10. Jamal U., Christine M., James H. et al. // *Organometallics.* – 2006. – **25**, N 23. – P. 5566.
11. *Amsterdam Density Functional (ADF) program*, Release 2005.02, Vrije Universiteit, Amsterdam, The Netherlands, 2007.
12. Stefan M., Julian H., Birger D. et al. // *J. Phys. Chem. A.* – 2009. – **113**, N 29. – P. 8366.
13. Vosko S.H., Wilk L., Nusair M. // *Can. J. Phys.* – 1980. – **58**. – P. 1200.
14. (a) Perdew J.P. // *Phys. Rev. B.* – 1986. – **33**. – P. 8822; (b) Becke A.D. // *Phys. Rev. A.* – 1988. – **38**. – P. 3098; (c) Perdew J.P. // *Phys. Rev. B.* – 1986. – **33**. – P. 8822.
15. (a) Lee C., Yang W., Parr R. // *Phys. Rev. B.* – 1988. – **37**. – P. 785; (b) Becke A.D. // *Phys. Rev. A.* – 1988. – **38**. – P. 3098; (c) Lee C., Yang W., Parr R.G. // *Phys. Rev. B.* – 1988. – **37**. – P. 785; (d) Johnson B.G., Gill P.M.W., Pople J.A. // *J. Chem. Phys.* – 1993. – **98**. – P. 5612; (e) Russo T.V., Martin R.L., Hay P.J. // *J. Chem. Phys.* – 1994. – **101**. – P. 7729.
16. Lenthe E., Baerends E.J., Snijders J.G. // *J. Chem. Phys.* – 1993. – **99**, N 6. – P. 4597; *J. Chem. Phys.* – 1994. – **101**, N 11. – P. 9783; *J. Chem. Phys.* – 1999. – **110**, N 18. – P. 8943.
17. Kohout M. DGrid, release 4.5 – Radebeul, 2009.
18. Chemcraft, release 1.4., <http://www.chemcraftprog.com/>

19. (a) *Fuentealba P., Savin A.* // *J. Phys. Chem. A.* – 2000. – **104**, N 46. – P. 10882; (b) *Kohout M., Savin A.* // *J. Comput. Chem.* – 1997. – **18**, N 12. – P. 1431.
20. *Bader R.F.W.* *Atoms in Molecules A quantum theory.* – UK, Oxford: Clarendon Press, 1990.
21. (a) *Popelier P.L.A., Logothetis G.* // *J. Organomet. Chem.* – 1998. – **555**, N 1. – P. 101; (b) *Thakur T.S., Desiraju G.R.* // *J. Mol. Struct. (Theochem.)*. – 2007. – **810**, N 1-3. – P. 143; (c) *Bader R.F.W.* *Atoms in Molecules A quantum theory.* – UK, Oxford: Clarendon Press, 1990.
22. *Novozhilova I.V., Volkov A.V., Coppens P.* // *Inorgan. Chem.* – 2004. – **43**, N 7. – P. 2299.
23. (a) *Cremer D., Kraka E.* // *Croat. Chem. Acta.* – 1984. – **57**. – P. 1259; (b) *Novozhilova I.V., Volkov A.V., Coppens P.* // *J. Amer. Chem. Soc.* – 2002. – **125**, N 4. – P. 1079.
24. (a) *Macci P., Sironi A.* // *Coord. Chem. Rev.* – 2003. – **238-239**. – P. 383; (b) *Espinosa E., Alkorta I., Elguero J., Molins E.* // *J. Chem. Phys.* – 2002. – **117**, N 12. – P. 5529; (c) *Mebis S., Henn J., Dittrich B. et al.* // *J. Phys. Chem. A.* – 2009. – **113**, N 29. – P. 8366.
25. *Marabello D., Bianchi R., Gervasio G., Cargnoni F.* // *Acta Cryst A.* – 2004. – **60**. – P. 494.
26. *Bader R.F.W., Essén H.* // *J. Chem. Phys.* – 1984. – **80**, N 5. – P. 1943.
27. *Espinosa A., Alkorta L., Elguero J., Molins E.* // *J. Chem. Phys.* – 2002. – **117**, N 12. – P. 5529.
28. *Egorova A.N., Tsirelson V.G.* // *Russ. J. Inorgan. Chem.* – 2006. – **51**, N 6. – P. 941.
29. *Carles B., Costas M., Poblet J.M. et al.* // *Inorg. Chem.* – 1996. – **35**, N 11. – P. 298.
30. *Carbo J.J., Crochet P., Esteruelas M.A. et al.* // *Organometallics.* – 2002. – **21**, N 2. – P. 305.
31. (a) *Ritchie J.P., Bachrach S.M.* // *J. Amer. Chem. Soc.* – 1987. – **109**, N 20. – P. 5909; (b) *Dem'yanov P.I., Gschwind R.M.* // *Organometallics.* – 2006. – **25**, N 24. – P. 5709.
32. *Loncke P.G., Pestherbe H.G.* // *J. Phys. Chem. A.* – 2004. – **108**, N 20. – P. 4694.
33. *Becke A.D., Edgecombe K.E.* // *J. Chem. Phys.* – 1990. – **92**, N 9. – P. 5397.
34. *Andrés J., Berski S., Feliz M. et al.* // *C. R. Chimie.* – 2005. – **8**, N 9-10. – P. 1400.
35. *Silvi B.* // *J. Mol. Struct. (Theochem.)*. – 2002. – **614**, N 1-3. – P.3.
36. (a) *Boily J.F.* // *J. Phys. Chem. A.* – 2003. – **107**, N 27. – P. 4276; (b) *Penka E. et al.* // *Inorgan. Chem.* – 2008. – **47**, N 1. – P. 42.
37. *Thomas F.F.* // *Chem. Soc. Rev.* – 2003. – **32**. – P. 80.